Chem Biol Drug Des 2011; **78:** 800–809

Research Article

doi: 10.1111/j.1747-0285.2011.01178.x

Synthesis, Antifungal Activity, and Docking Study of Some New 1,2,4-triazole Analogs

Jaiprakash N. Sangshetti, Deepak K. Lokwani, Aniket P. Sarkate and Devanand B. Shinde*

Department of Chemical Technology, Dr Babasaheb Ambedkar Marathwada, University, Aurangabad-431004 (MS), India
**Corresponding author: Devanand B. Shinde, dbsjaiprakash05@rediffmail.com*

Synthesis of new series of 1,2,4-triazole with 1,2,3-triazole and piperidine ring using $ZrOCl_2 \cdot 8H_2O$ as a catalyst in ethanol has been described. The yields obtained are in the range of 80–85%. All the synthesized compounds (3a–3o) are novel and were evaluated for their *in vitro* antifungal activities using standard agar method. Docking study of the newly synthesized compounds was performed, and results showed that all new compounds have similar binding mode in the active site of fungal enzyme P450 cytochrome lanosterol 14α-demethylase.

Key words: 1,2,3-triazole, 1,2,4-triazole, antifungal agents, docking study, structure–activity relationships

Received 14 October 2010, revised 1 July 2011 and accepted for publication 2 July 2011

1,2,4-triazole system and its analogs have been investigated as therapeutically interesting drug candidates because of their varied properties, such as selective COX-2 inhibitors (1), anti-acetylcholinesterase (2), and antimicrobial agents (3–6). The efficacy of anastrozole and letrozole as aromatase inhibitors and their use as nonsteroidal drugs for the treatment of estrogen-dependent cancer as well as the anticancer properties of ribavirine led to the investigation of many 1,2,4-triazole derivatives in laboratorial conditions for their antitumor activity (7,8). 1,2,4-triazole forms important part of many currently used azole antifungal agents (9,10). The most common approach to synthesize 1,2,4-triazole nucleus is from acyl hydrazide under basic or acidic condition.

In fungi, lanosterol 14α-demethylase ($P450_{14DM}$, CYP51), member of cytochrome P450 superfamily, is essential requirement for fungal viability (11). Lanosterol 14α-demethylase catalyzes removal of a methyl group at position C_{14} in the sterol molecule, which is a key step in ergosterol synthesis in fungi (12). Because CYP51s play a key role in fungal sterol biosynthetic pathways, they have been important targets for antifungal inhibitor design (9), such as CYP51s from *Candida albicans* (13,14), *Mycobacterium tuberculosis* (15–17), and *Penicillium digitatum* (18). The azoles have been found as one category of successful broad spectrum sterol 14α-demethylase inhibitors that selectively inhibit this enzyme causing depletion of ergosterol and accumulation of lanosterol and some other 14-methyl sterols and results in growth inhibition of fungal cell (9,19,20). The azole antifungal agents such as miconazole, fluconazole, and ketoconazole (Figure 1) act by mechanism in which heterocyclic nitrogen atom binds to heme iron atom in the active site of enzyme (21,22).

The series of antifungal agents containing 1,2,3-triazole and piperidine ring with 1,2,4-oxadiazole ring and 1,2,4-triazine ring were designed and synthesized in our group (23,24). Several compounds have been proved to have antifungal activity. Therefore, the chemical and biological features of the 1,2,3-triazole with piperidine derivatives provoked our strong interest for a further structure-activity relationship (SAR) study. In this study, we retain both 1,2,3-triazole and piperidine ring and replaces the 1,2,4-oxadiazole and 1,2,4-triazine ring with 1,2,4-triazole ring. On the basis of this strategy, we report here the synthesis and antifungal activity of the new series of 1,2,4-triazole derivatives coupled with 1,2,3-triazole ring. To get insight into binding of these azole compounds to fungal enzyme lanosterol 14α-demethylase, we carried out docking studies.

Experimental Section

General procedure for synthesis of 3a–3o

To a stirred mixture of hydrazides **1a–1o** (10 mmol), substituted aldehydes (10 mmol), ammonium acetate (40 mmol) in 15 mL ethanol was added $ZrOCl_2$ (2 mmol). The reaction mixture was heated under reflux for 12–13 h. After completion (Monitored by TLC), distilled water was added to the mixture and then extracted with three portions of ethyl acetate. The combined organic layers were washed with water. The organic layer on drying (Na_2SO_4) and concentrating in vacuo gave the desired compounds **3a–3o**. The experimental data showing period of reaction, % yield, molecular formula, and weight and elemental analysis of all synthesized compounds are depicted in Table S1 in supporting information.

Tert-butyl-(4-(5-phenyl-4*H*-1,2,4-triazol-3-yl)-1*H*-1,2,3-triazol-1-yl)piperidine-1-carboxylate (3a)

Off white solid; m. p. 201–202 °C.

^{1}H NMR (400 MHz, $CDCl_3$): δ = 8.20(s, 1H), 7.80–7.48 (m, 5H), 7.35 (s, 1H), 4.90–4.81 (m, 1H), 4.30–4.26 (m, 2H), 2.98–2.82 (m, 2H), 2.25–2.17 (m, 2H), 2.10–1.88 (m, 2H), 1.44 (s, 9H).

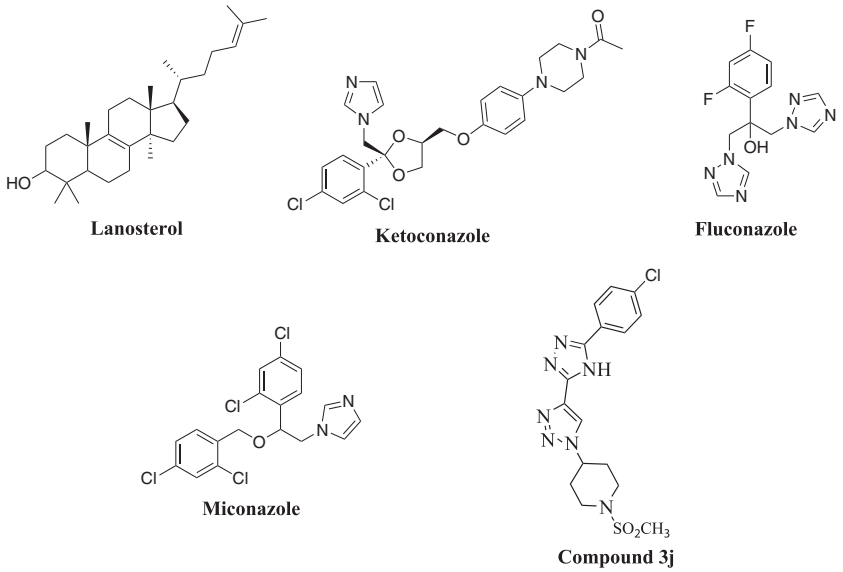

Figure 1: Chemical structures of lanosterol, ketoconazole, fluconazole, miconazole, and compound **3j**.

^{13}C NMR ($CDCl_3$) δ = 26.4, 28.8, 45.0, 60.5, 81.2, 126.3, 128.0, 130.4, 131.4, 133.2, 158.7, 162.5, 166.2

ES-MS: *m/z* = 397 $[M+H]^+$.

4-(4-(5-phenyl-4H-1,2,4-triazol-3-yl)-1*H*-1,2,3-triazol-1-yl)piperidine (3b)

Brown colored liquid; b.p. 201–202 °C.

^{1}H NMR (400 MHz, $CDCl_3$): δ = 9.15 (s, 1H), 8.22 (s, 1H), 7. 58–7. 35 (m, 5H), 7.15 (s, 1H), 4.76–4.61 (m, 1H), 4.53–4. 25 (m, 2H), 2.96–2.85 (m, 2H), 2.22–2.19 (m, 2H), 2.01–1.85 (m, 2H).

^{13}C NMR ($CDCl_3$) δ = 29.8, 44.2, 60.2, 81.2, 126.0, 129.1, 132.1, 133.2, 161.9, 165.4

ES-MS: *m/z* = 297$[M+H]^+$.

1-methyl-4-(4-(5-phenyl-4H-1,2,4-triazol-3-yl)-1*H*-1,2,3-triazol-1-yl)piperidine (3c)

Yellow solid; m.p. 211–212 °C.

^{1}H NMR (400 MHz, $CDCl_3$): δ = 7.90 (s, 1H), 7.78–7. 42 (m, 5H), 7.30 (s, 1H), 4.88–4.81 (m, 1H), 4.32–4.28 (m, 2H), 3.25 (s, 3H), 2.90–2.84(m, 2H), 2. 65–2.30 (m, 2H), 2.12–1.92 (m, 2H).

^{13}C NMR ($CDCl_3$) δ = 27.9, 49.1, 55.4, 60.7, 126.0, 129.1, 130.8, 132.1, 133.2, 160.8, 164.2

ES-MS: *m/z* = 310$[M+H]^+$.

1-ethyl-4-(4-(5-phenyl-4H-1,2,4-triazol-3-yl)-1*H*-1,2,3-triazol-1-yl)piperidine (3d)

Yellow solid; m.p. 189–190 °C.

^{1}H NMR (400 MHz, $CDCl_3$): δ = 7.95 (s, 1H), 7.71–7.41 (m, 5H), 7.34 (s, 1H), 4.90–4.85 (m, 1H), 4.44–4. 39 (q, 2H), 4.30–4.26 (m, 2H), 3.10–2.90 (m, 2H), 2.26–2.20 (m, 2H), 2.12–1.90 (m, 2H), 1.40–1.37 (t, 3H).

^{13}C NMR ($CDCl_3$) δ = 14.7, 26.5, 52.2, 54.4, 60.9, 126.0, 129.1, 130.5, 132.1, 133.2, 161.3, 163.6.

ES-MS: *m/z* = 324 $[M+H]^+$.

1-(methylsulfonyl)-4-(4-(5-phenyl-4H-1,2,4-triazol-3-yl)-1*H*-1,2,3-triazol-1-yl)piperidine (3e)

Off white solid; m.p. 201–202 °C.

^{1}H NMR (400 MHz, $CDCl_3$): δ = 8.15 (s, 1H), 7.79–7. 45 (m, 5H), 7.35 (s, 1H), 4.89–4.80 (m, 1H), 4.35–4.28 (m, 2H), 3.25 (s, 3H), 2.98–2.88 (m, 2H), 2.68–2.30 (m, 2H), 2.10–1.85 (m, 2H).

^{13}C NMR ($CDCl_3$) δ = 25.9, 42.2, 44.4, 60.1, 126.0, 129.1, 130.5, 132.1, 135.2, 162.3, 166.4

ES-MS: *m/z* = 374 $[M+H]^+$.

Phenyl(4-(4-(5-phenyl-4H-1,2,4-triazol-3-yl)-1*H*-1,2,3-triazol-1-yl)piperidine-1-yl)methanone (3f)

Off white solid; m.p. 209–211 °C.

^{1}H NMR (400 MHz, $CDCl_3$): δ = 8.20 (s, 1H), 7.90–7.45(m, 10H), 7.30 (s, 1H), 4.85–4.75(m, 1H), 4.15–4.05 (m, 2H), 2.95–2.84 (m, 2H), 2.19–2.12 (m, 2H), 1.88–1.80 (m, 2H).

^{13}C NMR ($CDCl_3$) δ = 26.8, 43.2, 59.8, 126.2,127.1, 128.6, 129.1, 130.6, 130.9, 131.8, 132.1, 137.4, 161.9, 165.3,173.2.

ES-MS: *m/z* = 400 $[M+H]^+$.

(4-chlorophenyl)(4-(4-(5-phenyl-4H-1,2,4-triazol-3-yl)-1*H*-1,2,3-triazol-1-yl)piperidine-1-yl)methanone (3g)

Yellowish solid; m.p. 174–175 °C.

^{1}H NMR (400 MHz, $CDCl_3$): δ = 8.15 (s, 1H), 7.85–7.36 (m, 9H), 7.29 (s, 1H), 4.82–4.73(m, 1H), 4.10–4.00 (m, 2H), 2.90–2.82 (m, 2H), 2.10–2.05 (m, 2H), 1.84–1.80 (m, 2H).

^{13}C NMR ($CDCl_3$) δ = 27.1, 42.9, 59.7, 126.6,128.2, 128.7, 129.2, 130.0, 130.8, 131.7, 132.4, 136.8, 161.9, 165.6,172.0.

ES-MS: *m/z* = 434[M+H]$^+$.

4-(4-(5-(4-chlorophenyl)-4H-1,2,4-triazol-3-yl)-1*H*-1,2,3-triazol-1-yl)-1-methylpiperidine (3h)

Yellowish solid; m.p. 224–226 °C.

^{1}H NMR (400 MHz, $CDCl_3$): δ = 8.10(s, 1H), 7. 80–7. 42 (m, 4H), 7.30 (s, 1H), 4.86–4.80 (m, 1H), 4.32–4.29 (m, 2H), 3.25 (s, 3H), 2.90–2.84 (m, 2H), 2. 60–2.32 (m, 2H), 2.10.1.90 (m, 2H).

^{13}C NMR ($CDCl_3$) δ = 26.8, 46.2, 56.2, 62.3, 126.4, 127.2, 129.1, 129.9, 131.2, 132.8, 133.1, 133.8, 137.1,162.2, 164.8.

ES-MS: *m/z* = 344 [M+H]$^+$.

1-(4-(4-(5-(4-chlorophenyl)-4H-1,2,4-triazol-3-yl)-1*H*-1,2,3-triazol-1-yl)piperidine-1-yl)ethanone (3i)

White solid; m.p. 267–269 °C.

^{1}H NMR (400 MHz, $CDCl_3$): δ = 7.95(s, 1H), 7.80–7.29 (m, 4H), 7.30 (s, 1H), 4.96–4.84 (m, 1H), 4.35–4.24 (m, 2H), 3.32(s, 3H), 2.92–2.88 (m, 2H), 2.64–2.32 (m, 2H), 2.12–1.85 (m, 2H). ES-MS: *m/z* = 372 [M+H]$^+$.

^{13}C NMR ($CDCl_3$) δ = 23.2, 28.2, 44.4, 61.8, 128.2, 130.1, 131.1, 132.2, 133.8, 134.3, 161.2, 173.8.

4-(4-(5-(4-chlorophenyl)-4H-1,2,4-triazol-3-yl)-1*H*-1,2,3-triazol-1-yl)-1-(methylsulfonyl)piperidine (3j)

Off white solid; m.p. 201–203 °C.

^{1}H NMR (400 MHz, $CDCl_3$): δ = 8.19 (s, 1H), 7.75–7.40 (m, 4H), 7.30 (s, 1H), 4.90–4.82 (m, 1H), 4.30–4.28 (m, 2H), 3.20 (s, 3H), 2.90–2.86 (m, 2H), 2.69–2.35 (m, 2H), 2.11–1.87 (m, 2H).

^{13}C NMR ($CDCl_3$) δ = 25.4, 42.7, 47.3, 60.4, 126.5, 129.6, 131.6, 132.4, 132.9, 133.1, 161.2, 165.7.

ES-MS: *m/z* = 409 [M+H]$^+$.

4-(4-(5-(4-methoxyphenyl)-4H-1,2,4-triazol-3-yl)-1*H*-1,2,3-triazol-1-yl)-1-methylpiperidine (3k)

Off white solid; m.p. 201–203 °C.

^{1}H NMR (400 MHz, $CDCl_3$): δ = 7.90 (s, 1H), 7.70–7.42 (m, 4H), 7.30 (s, 1H), 4.90–4.80 (m, 1H), 4.35–4.30 (m, 2H), 3.24 (s, 3H), 3.12 (s, 3H), 2.90–2.88 (m, 2H), 2. 68–2.32 (m, 2H), 2.10–1.88 (m, 2H).

^{13}C NMR ($CDCl_3$) δ = 27.8, 48.2, 56.1, 115.4, 126.1, 129.1, 131.2, 158.5, 162.1, 166.4.

ES-MS: *m/z* = 340[M+H]$^+$.

1-ethyl-4-(4-(5-(4-methoxyphenyl)-4H-1,2,4-triazol-3-yl)-1*H*-1,2,3-triazol-1-yl)piperidine (3l)

Off white solid; m.p. 201–203 °C.

^{1}H NMR (400 MHz, $CDCl_3$): δ = 8.10 (s, 1H), 7.80–7.42 (m, 4H), 7.35 (s, 1H), 4.90–4.85 (m, 1H), 4.45–4. 38 (q, 2H), 4.35–4.25 (m, 2H), 3.28 (s, 3H) 2.98–2.86 (m, 2H), 2.22–2.18 (m, 2H), 2.11–1.90 (m, 2H), 1.45–1.40 (t, 3H).

^{13}C NMR ($CDCl_3$) δ = 14.2, 28.2, 49.4, 56.3, 62.6, 116.2, 126.4, 129.8, 132.1, 157.9, 160.8, 166.4.

ES-MS: *m/z* = 354 [M+H]$^+$.

1-(methylsulfonyl)-4-(4-(5-(4-nitrophenyl)-4H-1,2,4-triazol-3-yl)-1*H*-1,2,3-triazol-1-yl)piperidine (3m)

Yellow solid; m.p. –189–190 °C.

^{1}H NMR (400 MHz, $CDCl_3$): δ = 8.15 (s, 1H), 7 72–7. 38 (m, 4H), 7.37 (s, 1H), 4.89–4.81 (m, 1H), 4.32–4.28 (m, 2H), 3.24 (s, 3H), 2.92–2.86 (m, 2H), 2.69–2.32 (m, 2H), 2.10–1.85 (m, 2H).

^{13}C NMR ($CDCl_3$) δ = 26.8, 40.4, 44.3, 61.6, 127.4, 129.4, 131.1,138.2, 157.6, 164.2

ES-MS: *m/z* = 419 [M+H]$^+$.

1-(4-(4-(5-p-tolyl-4H-1,2,4-triazol-3-yl)-1*H*-1,2,3-triazol-1-yl)piperidine-1-yl)ethanone (3n)

Off white solid; m.p. –201–202 °C.

^{1}H NMR (400 MHz, $CDCl_3$): δ = 8.20 (s, 1H), 7.80–7.35 (m, 4H), 7.30 (s, 1H), 4.93–4.82 (m, 1H), 4.34–4.28 (m, 2H), 3.32 (s, 3H), 2.91–2.87 (m, 2H), 2.87 (s, 3H), 2.65–2.35 (m, 2H), 2.10–1.90 (m, 2H).

^{13}C NMR ($CDCl_3$) δ = 22.2,23.4, 26.6, 41.8, 62.1, 124.2, 129.1, 131.1,132.5, 164.0

ES-MS: *m/z* = 352 [M+H]$^+$.

***Phenyl(4-(4-(5-p-tolyl-4H-*1,2,4-triazol-3-yl)-1*H-*1,2,3-triazol-1-yl)piperidine-1-yl)methanone (3o)**

Yellow solid; m.p. –211–212 °C.

^{1}H NMR (400 MHz, $CDCl_3$): δ = 8.20(s, 1H), 7.90–7.38 (m, 9H), 7.39 (s, 1H), 4.80–4.75(m, 1H), 4.10–4.05 (m, 2H), 3.32 (s, 3H), 2.95–2.85(m, 2H), 2.20–2.11 (m, 2H), 1.84–1.80 (m, 2H).

^{13}C NMR ($CDCl_3$) δ = 21.7, 26.3, 42.6, 61.2, 124.7, 126.4, 129.4,130.3, 131.41,132.7, 136.8, 158.5, 164.3,173.0.

ES-MS: m/z = 415 $[M+H]^+$.

Antifungal activity

The antifungal activity was evaluated against different fungal strains, such as *C. albicans*, *Fusarium oxysporum*, *Aspergillus flavus*, *Aspergillus niger*, and *Cryptococcus neoforman*. Minimum inhibitory concentration (MIC) values were determined using standard agar method (25–27). Miconazole and Fluconazole were used as a standard for the comparison of antifungal activity. Dimethyl sulfoxide was used as solvent control.

Computational methods

The 3D model structure of cytochrome P450 lanosterol 14α-demethylase of *C. albicans* was built using homology modeling. Amino acid sequence of enzyme was obtained from the Universal Protein Resource (http://www.uniprot.org/) (Accession Code: P10613), and sequence homologous was obtained from Protein Data Bank (PDB) using Blast search. In literature, the structure of cytochrome P450 lanosterol 14α-demethylase was developed homologically using crystal structure of lanosterol 14α-demethylase from *M. tuberculosis* as template (5,28–31). Based on the result of blast search, we used the crystal structure of human lanosterol 14-α DM (CYP51) with ketoconazole as a template for homology modeling (PDB ID. 3I3K). A hidden Markov model (HMM) was generated from a sequence alignment for the identification of sequence motifs and query family, which provides the information about which residues are conserved in the consensus sequence. This information was used as constraints in the generation of the protein sequence alignment. In addition, secondary structure prediction algorithms SSpro (32) were used for alignment of *C. albicans* lanosterol 14α-demethylase to human lanosterol 14α-demethylase enzyme. The combination of sequence motifs and secondary structure provides accurate picture of each helix. Alignment of *C. albicans* lanosterol 14α-demethylase with human lanosterol 14α-demethylase enzyme was carried out using the automated alignment program in PRIME v2.1 (Schrödinger, LLC, New York, NY, USA). Following automated alignment, manual inspection was made to ensure the conserved motifs, and loops were correctly aligned. The final model of *C. albicans* lanosterol 14-α DM enzyme was developed using PRIME v2.1. The binding sites were generated using SITEMAP v2.3 (33) (Schrödinger), and side chain and loops around active binding site (site with highest sitemap score) were refined using Prime refinement tool. The quality of generated *C. albicans* lanosterol 14α-demethylase model was assessed by using the well-validated programs PROCHECK (34) and WHATIF (35).

The developed protein was further preprocessed, optimized, and minimized to 0.3 RMSD using 'protein preparation wizard' in MAESTRO v9.0 (Schrödinger). In the human lanosterol 14α-demethylase X-ray structure, ketoconazole binds with its azole ring perpendicular to the heme porphyrin plane and with N-4 of the triazole co-ordinated to the heme iron. Therefore, constraints were defined that triazole rings of all synthesized compounds overlapped the ketoconazole triazole. At last, grids were generated around active site of enzyme by centering them on the ligand using default box size. The structure of all compounds was built using Maestro build panel and prepared by LIGPREP v2.3 (Schrödinger) module, which produces lower energy conformers of all compounds using OPLS_2005 force field. In Ligprep module, the Epik 2.0 program (36) was used for generation of ionized state of all compounds at target pH 7.0 ± 2.0. The lower energy conformers were selected and docked into grid generated from protein structure using Standard Precision (SP) docking mode in molecular docking tool, GLIDE v5.5 (37) (Schrödinger). The final evaluation of ligand–protein binding was carried out with Glide score (docking score).

G (GLIDE) score = $a \times$ vdW + $b \times$ Coul + Lipo + H bond + Metal + BuryP + Rot B + Site

where vdW, van der Waals energy; Coul, Coulomb energy; Lipo, Lipophilic contact term; HBond, Hydrogen-bonding term; Metal, Metal-binding term; BuryP, Penalty for buried polar groups; RotB, Penalty for freezing rotatable bonds; Site, Polar interactions at the active site; and the coefficients of vdW and Coul are a = 0.065 and b = 0.130.

Results and discussion

Chemistry

The syntheses of compounds **3a–3o** are outlined in Scheme 1. Starting hydrazide compound has been prepared as reported in our previous work (24). Corresponding hydrazide compounds **1a–1o**, ammonium acetate, and aromatic aldehydes were heated under reflux in ethanol using 20 mol% $ZrOCl_2{\cdot}8H_2O$ to get the target compounds **3a–3o** (Scheme 1). Catalytic property of $ZrOCl_2$ has been studied considering synthesis of **3a**. Effects of various solvents like *THF*, acetonitrile, and ethanol have also been studied (Table 1). Among the results obtained, use of 20-mol% $ZrOCl_2$ in ethanol gave the better yield (85%) for the synthesis of **3a**. The synthetic procedure was extended for synthesis of all the compounds **3a–3o** using different hydrazides and aromatic aldehydes. The yields were obtained in the range of 80–85% (see Supporting Information). All synthesized derivatives were characterized using mass and ^{1}H NMR.

Antifungal activity and docking study

All the synthesized compounds were screened for *in vitro* antifungal activity. The antifungal activity was evaluated against different fungal strains. Minimum inhibitory concentration values of the tested compounds are presented in Table 2.

We found that introduction of 1,2,4-triazole ring in place of 1,2,4-oxadiazole ring and 1,2,4-triazine ring (reported previously)

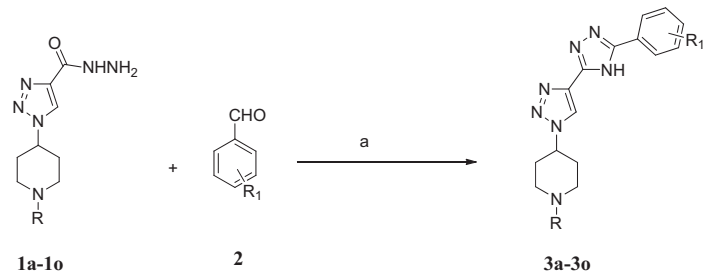

3a R = Boc R_1 = H **3b** R = H R_1 = H **3c** R = CH_3 R_1 = H **3d** RC_2H_5 R_1 = H
3e R = SO_2CH_3 R_1 = H **3f** R = COC_6H_5 R_1 = H **3g** R = COC_6H_5 4Cl R_1 = H **3h** R = CH_3 R_1 = 4Cl
3i R = $COCH_3$ R_1 = 4Cl **3j** R = SO_2CH_3 R_1 = 4Cl **3k** R = CH_3 R_1 = $4OCH_3$ **3l** R = C_2H_5 R_1 = $4OCH_3$
3m R = SO_2CH_3 R_1 = $4NO_2$ **3n** R = $COCH_3$ R_1 = $4CH_3$ **3o** R = COC_2H_5 R_1 = $4CH_3$

Scheme 1: Synthesis of series of new 1,2,4-triazole analogs. (a) 20 mol% $ZrOCl_2 \cdot 8H_2O$, NH_4OAc, EtOH.

Table 1: Optimization of reaction conditions and the quantity of $ZrOCl_2$ for the synthesis of *tert*-butyl-(4-(5-phenyl-4*H*-1,2,4-triazol-3-yl)-1*H*-1,2,3-triazol-1-yl) piperidine-1-carboxylate (**3a**)

Solvent	Mol% of $ZrOCl_2$	Reaction time (h)	Yield[a] (%)
THF	20	24	58
Acetonitrile	20	24	60
Dichloromethane	20	20	55
Ethanol	20	12	85
Ethanol	10	12	74

[a]Yields refer to the isolated pure products.

maintains and increases the antifungal activity against all tested organism except *Cryptococcus neoformans*. It was also observed that orders of antifungal activity against all tested organism appeared to be $-SO_2CH_3 > CH_3 > C_2H_5$ substitution on piperidine ring, consistent with our previous observations.

From the antifungal activity data (Table 2), it is observed that compounds **3e**, **3h**, and **3j** are the most active among all tested compounds. *N*-protected compound with phenyl substituents at five position (**3a**) shows diminished antifungal activity compared to miconazole and fluconazole. Deprotected compound **3b** shows significant rise in activity compared to **3a**. Substitution of methyl group (**3c**) on piperidine nitrogen increases the antifungal activity compared with unsubstituted nitrogen (**3b**). Activity of compound **3c** was comparable with miconazole against C. *albicans* and *F. oxysporum*. Substitution of ethyl group (**3d**) on nitrogen reduces the activity against all tested organisms except *C. neoformans* where it shows slight increase in activity compared with methyl-substituted analog. Introduction of mesyl group on nitrogen (**3e**) increases the antifungal activity compared with unsubstituted piperidine against all tested organisms. Compound **3e** was more potent against *C. albicans* compared with miconazole whereas equipotent with miconazole against *F. oxysporum*. Introduction of benzoyl or *p*-chloro

Table 2: Antifungal activity and results of docking study of the synthesized compounds

Compound	MIC values in μg/mL					*G*-score	Distance between N of azole and Heme ring (Å)
	Candida albicans	*Fusarium oxysporum*	*Aspergillus flavus*	*Aspergillus niger*	*Cryptococcus neoformans*		
3a	160	100	120	*	*	−6.60	2.9
3b	50	40	40	70	60	−6.13	3.2
3c	30	30	30	50	150	−6.30	3.0
3d	45	40	40	60	120	−7.18	3.3
3e	20	25	30	40	100	−6.88	3.2
3f	100	*	160	*	180	−7.78	3.7
3g	120	160	*	*	100	−8.01	3.3
3h	25	25	30	40	*	−6.19	3.2
3i	30	40	50	50	*	−6.34	3.2
3j	20	20	20	30	*	−6.41	3.4
3k	30	30	40	20	150	−6.11	3.2
3l	60	70	70	50	*	−6.71	3.4
3m	30	40	40	30	*	−5.60	–
3n	80	70	50	35	140	−6.11	3.2
3o	160	*	180	*	*	−6.26	3.2
Miconazole	25	25	12.5	12.5	25	−7.33	2.4
Fluconazole	5	5	5	10	5	−5.02	2.7
Ketoconazole	–	–	–	–	–	−6.83	2.6

*No activity was observed up to 200 μg/mL.
[a]Values are the average of three readings.

benzoyl group on nitrogen (**3f**, **3g**) shows significant loss of activity compared with unsubstituted nitrogen.

Introduction of *-Cl* group on 5-phenyl (**3h–3j**) shows increase in activity against all tested organisms except *C. neoformans* compared to compounds with unsubstituted 5-phenyl group. Compound **3h** was equipotent with miconazole against *F. oxysporum* and *C. albicans*. Activity of Compound **3i** was comparable with miconazole against *C. albicans*. Compound **3j** with methyl sulfone group on piperidine nitrogen and *-Cl* group on five phenyl substituents was more potent against *F. oxysporum* and *C. albicans* than miconazole. Introduction of *-OCH_3* group on 5-phenyl (**3k**) with *–CH_3* group on piperidine does not affect the activity against *C. albicans* and *F. oxysporum*, whereas it increases against *A. niger* compared to compounds with unsubstituted 5-phenyl group. Introduction of *-NO_2* group on 5-phenyl with *-SO_2CH_3* on piperidine (**3m**) shows decrease in activity against all tested organisms compared to compounds with unsubstituted 5-phenyl group. Introduction of *CH_3* group on 5-phenyl (**3n**, **3o**) shows decrease in activity against all tested organism compared to **3f** and **3i**. In conclusion, compounds **3e** and **3j** were the most potent compound from the series.

In addition, we developed the homology model of cytochrome P450 lanosterol 14α-demethylase of *C. albicans*. The crystal structure of human lanosterol 14α-demethylase with ketoconazole was used as template for homology model, and sequence identity between human and *C. albicans* lanosterol 14α-demethylase was found 34%. Alignment of *C. albicans* lanosterol 14α-demethylase with human lanosterol 14α-demethylase enzyme is shown in Figure 2. The final model was generated with Prime (Figure 3). The final statistical analysis of the Ramachandra plot showed that 91.9% of the main chain dihedral angles were found in the most favorable region, thus confirming the good quality of the generated 3D model. The binding sites in *C. albicans* lanosterol 14α-demethylase enzyme were indentified using Sitemap. The binding cavity with best sitescore (Sitescore-1.122) containing hydrophobic, metal-binding, and hydrogen

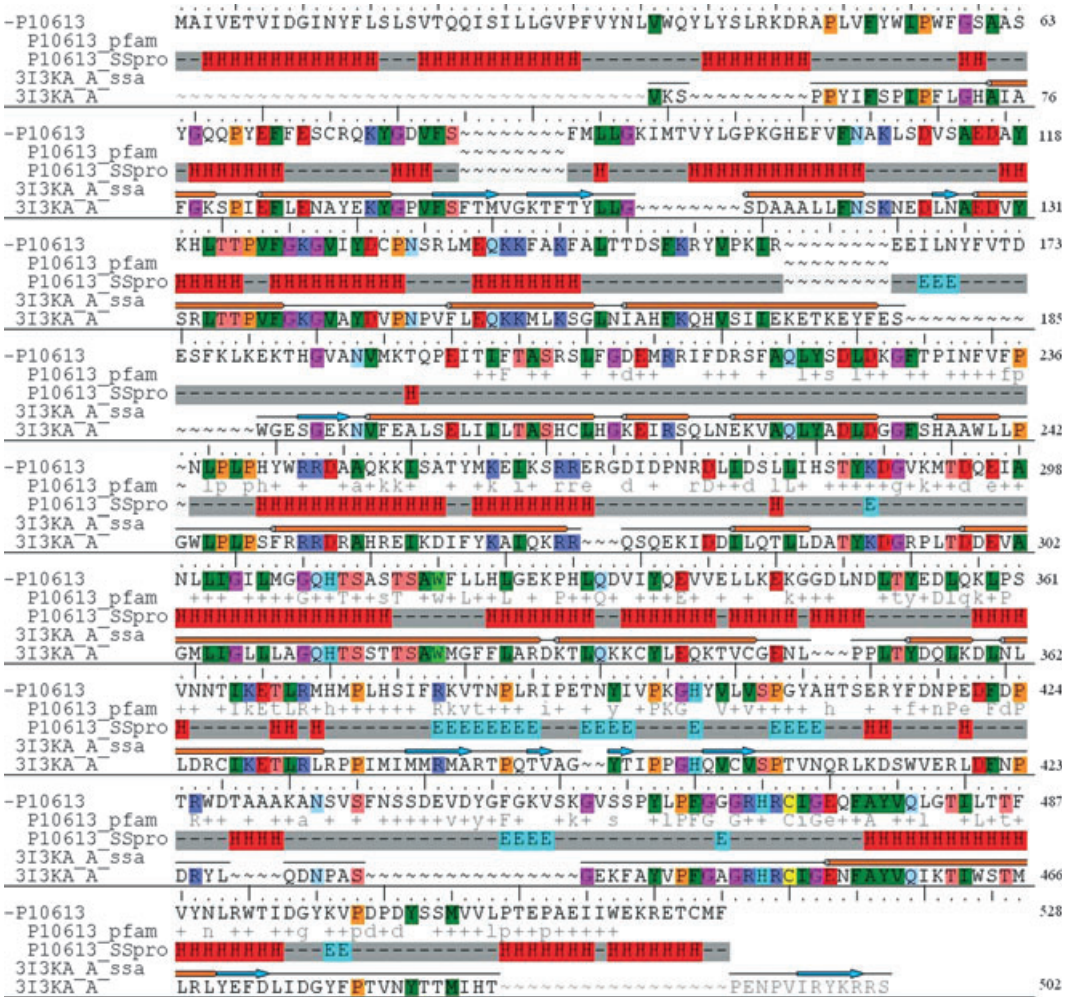

Figure 2: Alignment of amino acid sequence of CA-CYP51 (P10613) and human CYP51 (3I3K_A). Key: pfam, predicted family by HMM consensus sequence; capital letters, highly conserved region; lowercase letter, matches HMM; (+) match is conservative according to HMM; SSPro, Secondary structure prediction; H, alpha helix; E, beta strand; (–) loop; ssa, secondary structure assignment; red cylinder, alpha helix; cyan arrow, beta strand; black line – loop.

Figure 3: Structure of homology model of CA-CYP51. Helices and strands are highlighted in red and cyan color. The heme cofactor is highlighted in green.

acceptor region was obtained around position of ligand and heme (Figure 4). A subunit above heme ring represents metal-binding space and hydrophobic area. Hydrophobic scaffolds of the inhibitors (such as the sterol group of the substrate) or groups that co-ordinate with the heme (such as the triazole or imidazole group of the azole inhibitors) are favorable in this pocket.

The docking study was also performed to study and predict the binding mode of newly synthesized compounds with the target enzyme cytochrome P450 lanosterol 14α-demethylase of *C. albicans*. All compounds showed similar docking mode in the active site of the enzyme. The 1,2,4-triazole ring (compounds **3a**, **3d**, **3e**, **3g**, **3i–3l**, and **3n**) or 1,2,3-triazole ring (compounds **3b**, **3c**, **3f**, **3h**, and **3o**) is positioned almost perpendicular to the porphyrin plane, with a ring nitrogen atom co-ordinated to the heme iron (Figure 5). The distance between nitrogen of azole ring in all compounds and heme ring was measured and found in the range of 2.9–3.7 Å and was comparable with that found in the crystal structure of human lanosterol 14α-demethylase complexed with azole inhibitors (Table 2). In the most of the compounds, phenyl ring occupied the same hydrophobic region above the heme ring and showed good van der Waals interaction with heme and amino acids PHE126, ILE131, LEU300, and ILE304, whereas piperidine ring of most of compounds located in same hydrophobic region by making good van der Waals interaction with TYR118, LEU121, PHE228, LEU376, and MET508. In particular, all hydrophobic substituents find location in a hydrophobic subsite above the heme ring.

Docking score (*G*-score) of all compounds are shown in Table 2. The good *in vitro* activity of compounds **3e**, **3j**, **3h, 3c, 3i,** and **3k** is ascribed to their strong binding affinity for *C. albicans* lanosterol 14α-demethylase enzyme shown by docking score. The higher docking score of compounds **3g, 3f, 3o, 3a, and 3l** is linked to their long side chain that fits into the binding cavity of *C. albicans*

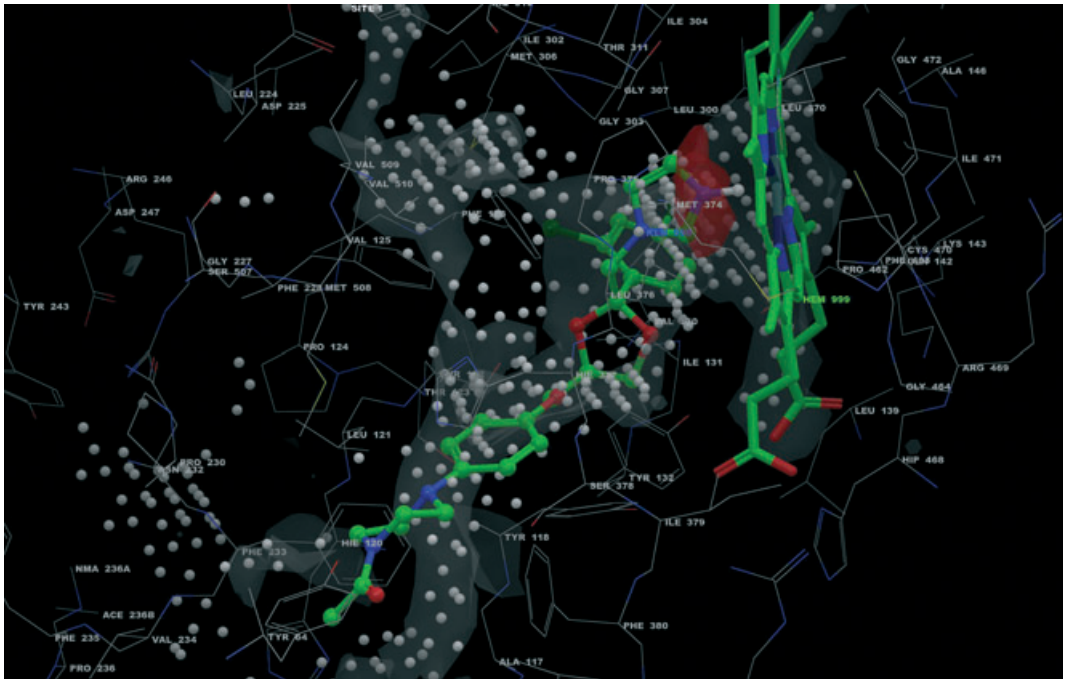

Figure 4: Site points, hydrophobic, and metal-binding region for enzyme. The protein is shown in wireframe.

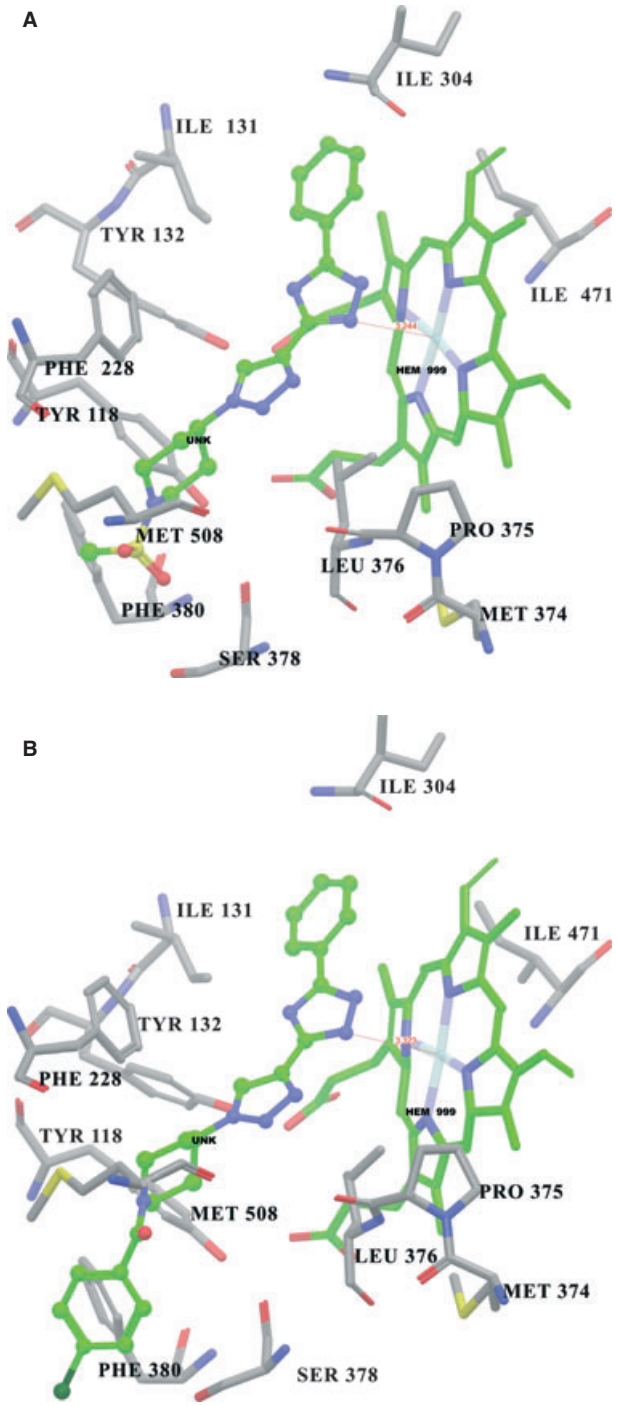

Figure 5: Binding mode of compounds (A) **3e** and (B) **3g** in active site of cytochrome P450 lanosterol 14α-demethylase of *Candida albicans*. The distance of nitrogen of azole ring and heme ring is indicated in red dotted line. The hydrogen atoms are removed for clarity.

lanosterol 14α-demethylase enzyme, but showed weak *in vitro* activity. The low docking score of compounds **3b** and **3n** is associated with their bad van der Waals interaction with heme ring. The low docking score of compound **3m** is linked with its pose, triazole ring not perpendicular to heme iron.

Conclusion

Synthesis of a novel series of 1,2,4-triazole with 1,2,3-triazole and piperidine ring has been demonstrated. Based on the activity data, SAR for the series has been developed. From SAR, it can be said that compounds **3e** and **3j** are most active compounds from the series, thus suggesting that the present series containing 1,2,4-triazole with 1,2,3-triazole and piperidine ring with methyl sulfone group on piperidine nitrogen can serve as important pharmacophore for the design of new antifungal agent with potent activity. Docking study of all compounds in active site of enzyme cytochrome P450 lanosterol 14α-demethylase of *C. albicans* has been carried out. From their binding mode, it can be suggested that 1,2,4-triazole and 1,2,3-triazole rings in present series serve as necessary requirement for good interaction with heme iron for inhibition of enzyme and potential antifungal activity.

Acknowledgments

The authors are thankful to Council for Scientific and Industrial Research (CSIR), New Delhi, for financial assistance. The authors are thankful to Principal, Maharashtra Institute of Pharmacy, Pune, for *in vitro* antifungal activity. The authors are also thankful to the Head, Department of Chemical Technology, Dr Babasaheb Ambedkar Marathwada University, Aurangabad 431 004 (MS), India, for providing the laboratory facility.

References

1. Navidpour L., Shafaroodi H., Abdi K., Amini M., Ghahremani M.H., Dehpour A.R., Shafiee A. (2006) Design, synthesis, and biological evaluation of substituted 3-alkylthio-4,5-diaryl-4*H*-1,2,4-triazoles as selective COX-2 inhibitors. Bioorg Med Chem;14:2507–2517.
2. Holan G., Virgona C., Watson K.G. (1997) Synthesis and anti-acetylcholinesterase activity of some 5-substituted 1-methyl-1H-1,2,4-triazol-3-yl methanesulfonates. Aust J Chem;50:153–158.
3. Matsumoto M., Ishida K., Konagai A., Maebashi K., Asaoka T. (2002) Strong antifungal activity of SS750, a new triazole derivative, is based on its selective binding affinity to cytochrome P450 of fungi. Antimicrob Agents Chemother;46:308–314.
4. Zamani K., Faghihi K., Tofighi T., Shariatzadeh M.R. (2004) Synthesis and antimicrobial activity of some pyridyl and naphthyl substituted 1,2,4-triazole and 1,3,4-thiadiazole derivatives. Turk J Chem;28:95–100.
5. Banfi E., Scialino G., Zampieri D., Mamolo M., Vio L., Ferrone M., Fermeglia M., Paneni M., Pric S. (2006) Antifungal and antimycobacterial activity of new imidazole and triazole derivatives. A combined experimental and computational approach. J Antimicrob Chemother;58:76–84.

6. Castagnolo D., Radi M., Dessi F., Manetti F., Saddi M., Meleddu R., De Logu A., Botta M. (2009) Synthesis and biological evaluation of new enantiomerically pure azole derivatives as inhibitors of *Mycobacterium tuberculosis*. Bioorg Med Chem Lett;19:2203–2205.
7. Marzano C., Pellei M., Colavito D., Alidori S., Lobbia G.G., Gandin V., Tisato F., Santini C. (2006) Synthesis, characterization, and *in vitro* antitumor properties of tris(hydroxymethyl) phosphine copper(I) complexes containing the new bis(1,2,4-triazol-1-yl)acetate ligand. J Med Chem;49:7317–7324.
8. Jackson T., Lawrence Woo L.W., Trusselle M.N., Chander S., Purohit A., Reed M.J. (2007) Dual aromatase–sulfatase inhibitors based on the anastrozole template: synthesis, *in vitro* SAR, molecular modelling and *in vivo* activity. Org Biomol Chem;5:2940–2952.
9. Sheehan D.J., Hitchcock C.A., Sibley C.M. (1999) Current and emerging azole antifungal agents. Clin Microbiol Rev;12:40–79.
10. Cools H.J., Fraaije B.A., Kim S.H., Lucas J. (2006) Impact of changes in the target P450 CYP51 enzyme associated with altered triazole sensitivity in fungal pathogens of cereal crops. Biochem Soc Trans;34:1219–1222.
11. Vanden Bossche H., Koymans L. (1998) Cytochrome P450 in fungi. Mycoses;41:32–38.
12. Yoshida Y., Aoyama Y., Noshiro M., Gotoh O. (2000) Sterol 14α-demethylase P450 (CYP51) provides a breakthrough for the discussion on the evolution of cytochrome P450 gene family. Biochem Biophys Res Commun;273:799–804.
13. Xu Y., Sheng C., Wanga W., Che X., Cao Y., Dong G., Wang S., Ji H., Miao Z., Yao J., Zhang W. (2010) Structure-based rational design, synthesis and antifungal activity of oxime-containing azole derivatives. Bioorg Med Chem Lett;20:2942–2945.
14. Rezaei Z., Khabnadideh S., Pakshir K., Hossaini Z., Amiri F., Assadpour E. (2009) Design, synthesis, and antifungal activity of triazole and benzotriazole derivatives. Eur J Med Chem;44:3064–3067.
15. Souter A., McLean K.J., Smith W.E., Munro A.W. (2000) The genome sequence of *Mycobacterium tuberculosis* reveals cytochromes P450 as novel anti-TB drug targets. J Chem Technol Biotechnol;75:933–941.
16. Guardiola-Diaz H.M., Foster L.A., Mushrush D., Vaz A.D. (2001) Azole antifungal binding to a novel cytochrome P450 from *Mycobacterium tuberculosis*: implications for treatment of tuberculosis. Biochem Pharmacol;61:1463–1470.
17. Munro A.W., McLean K.J., Marshall K.R., Warman A.J., Lewis G., Roitel O., Sutcliffe M.J., Kemp C.A., Modi S., Scrutton N.S., Leys D. (2003) Cytochromes P450: novel drug targets in the war against multidrug-resistant *Mycobacterium tuberculosis*. Biochem Soc Trans;31:625–630.
18. Hamamoto H., Hasegawa K., Nakaune R., Lee Y.J., Makizumi Y., Akutsu K., Hibi T. (2000) Tandem repeat of a transcriptional enhancer upstream of the sterol 14α-demethylase gene (CYP51) in *Penicillium digitatum*. Appl Environ Microbiol;66:3421–3426.
19. Ji H., Zhang W., Zhou Y., Zhang M., Zhu J., Song Y., Lu J., Zhu J. (2000) A three-dimensional model of lanosterol 14α-demethylase of *Candida albicans* and its interaction with azole antifungals. J Med Chem;43:2493–2505.
20. Che X., Sheng C., Wang W., Cao Y., Xu Y., Ji H., Dong G., Miao Z., Yao J., Zhang W. (2009) New azoles with potent antifungal activity: design, synthesis and molecular docking. Eur J Med Chem;44:4218–4226.
21. Ji H., Zhang W., Zhang M., Kudo M., Aoyama Y., Yoshida Y., Sheng C., Song Y., Yang S., Zhou Y., Lu J., Zhu J. (2003) Structure-based de novo design, synthesis, and biological evaluation of non-azole inhibitors specific for lanosterol 14α-demethylase of fungi. J Med Chem;46:474–485.
22. Strushkevich N., Usanov S.A., Park H. (2010) Structural basis of human CYP51 inhibition by antifungal azoles. J Mol Biol;397:1067–1078.
23. Sangshetti J.N., Nagawade R.R., Shinde D.B. (2009) Synthesis of novel 3-(1-(1-substituted piperidin-4-yl)-1H-1,2,3-triazol-4-yl)-1,2,4-oxadiazol-5(4H)-one as antifungal agents. Bioorg Med Chem Lett;19:3564–3567.
24. Sangshetti J.N., Shinde D.B. (2010) One pot synthesis and SAR of some novel 3-substituted 5,6-diphenyl-1,2,4-triazines as antifungal agents. Bioorg Med Chem Lett;20:742–745.
25. Saundane A.R., Rudresh K., Satynarayan N.D., Hiremath S.P. (1998) Pharmacological screening of 6H, 11H-indolo {3, 2-c} isoquinolin-5-ones and their derivatives. Indian J Pharm Sci;60:379–383.
26. Greenwood D., Slack R.C.B., Peutherer J.F. (1992) Medical Microbiology. London: ELBS.
27. Duraiswamy B., Mishra S.K., Subhashini V., Dhanraj S.A., Suresh B. (2006) Studies on the antimicrobial potential of *Mahonia leschenaultii* Takeda root and root bark. Indian J Pharm Sci;68:389–390.
28. Xiao Li., Madison V., Chau A.S., Loebenberg D., Palermo R.E., McNicholas P.M. (2004) Three-dimensional models of wild-type and mutated forms of cytochrome P450 14α-sterol demethylases from *Aspergillus fumigatus* and *Candida albicans* provide insights into posaconazole binding. Antimicrob Agents Chemother;48:568–574.
29. Sheng C., Miao Z., Ji H., Yao J., Wang W., Che X., Dong G., Lu J., Guo W., Zhang W. (2009) Three-dimensional model of lanosterol 14α-demethylase from *Cryptococcus neoformans*: active-site characterization and insights into azole binding. Antimicrob Agents Chemother;53:3487–3495.
30. Zhang Q., Li D., Wei P., Zhang J., Wan J., Ren Y., Chen Z., Liu D., Yu Z., Feng L. (2010) Structure-based rational screening of novel hit compounds with structural diversity for cytochrome P450 sterol 14α-demethylase from *Penicillium digitatum*. J Chem Inf Model;50:317–325.
31. Sheng C., Wang W., Che X., Dong G., Wang S., Ji H., Miao Z., Yao J., Zhang W. (2010) Improved model of lanosterol 14α-demethylase by ligand-supported homology modeling: validation by virtual screening and azole optimization. Chemmedchem;5:390–397.
32. Pollastri G., Przybylski D., Rost B., Baldi P.F. (2002) Improving the prediction of protein secondary structure in three and eight classes using recurrent neural networks and profiles. Proteins;47:228–235.
33. Halgren T. (2007) New method for fast and accurate binding-site identification and analysis. Chem Biol Drug Des;69:146–148.
34. Hooft R.W.W., Vriend G., Sander C., Abola E.E. (1996) Errors in protein structures. Nature;381:272.

35. Laskowski R.A., MacArthur M.W., Moss D., Thornton J.M. (1993) PROCHECK: a program to check the stereochemical quality of protein structures. J Appl Cryst;26:283–291.
36. Shelley J.C., Cholleti A., Frye L.L., Greenwood J.R., Timlin M.R., Uchiyama M. (2007) Epik: a software program for pKa prediction and protonation state generation for drug-like molecules. J Comput Aided Mol Des;21:681–691.
37. Friesner R.A., Banks J.L., Murphy R.B., Halgren T.A., Klicic J.J., Mainz D.T., Repasky M.P., Knoll E.H., Shelley M., Perry J.K., Shaw D.E., Francis P., Shenkin P.S. (2004) Glide: a new approach for rapid, accurate docking and scoring. 1. Method and assessment of docking accuracy. J Med Chem;47:1739–1749.

Supporting Information

Additional Supporting Information may be found in the online version of this article:

Table S1. Experimental data of the synthesized compounds **3a–3o**.

Please note: Wiley-Blackwell is not responsible for the content or functionality of any supporting materials supplied by the authors. Any queries (other than missing material) should be directed to the corresponding author for the article.